JOURNAL OF COMPUTATIONAL PHYSICS 5, 406–414 (1970)

Finite Difference Scheme for Calculating Problems in Two Space Dimensions and Time*

MARK L. WILKINS

Lawrence Radiation Laboratory, University of California, Livermore, California 94550

Received November 11, 1969

The effectiveness of a finite difference scheme for solving problems in continuum mechanics is demonstrated by a series of problems ranging from elasticity theory to gas dynamics. All of the results shown were plotted directly by the high speed computer and permit an easy evaluation of the technique.

In 1950 von Neumann and Richtmyer proposed the artificial viscosity method for calculating problems in hydrodynamics. The technique was described for one-dimensional flow with the Lagrange form of the hydrodynamic differential equations. The region of flow was divided into a finite mesh of grid points at which the various parameters could be specified. The differential equations were then approximated by a second-order-difference scheme involving these grid-point parameters. It was found that the quadratic artificial viscosity used by von Neumann and Richtmyer to treat shocks did not provide sufficient damping for non-physical oscillations that usually occurred in the grid. However, this difficulty is easily overcome by incorporating a linear viscosity to stabilize the grid. The result is a second-order-difference scheme that gives very accurate results for a large range of problems in one space dimension.

When the finite mesh and artificial viscosity concept is extended into two space dimensions, many different ways of formulating the differential equations and the finite difference equations result. Also, the additional degree of freedom in the mesh permits an increased possibility for nonphysical grid distortion, analogous to the non-physical oscillations in the one-dimensional problem. The problem of grid distortion plus the possibility of formulating the equations in many different ways has led to a search for the best method of solving problems in hydrodynamics using the original von Neumann–Richtmyer idea. One of the approaches taken is to damp spurious signals in the grid by including more grid points in the difference operators. One prescription for incorporating more grid points into the difference

* Work performed under the auspices of the U.S. Atomic Energy Commission.

equations is to include third-order terms in the difference operator. This implies that the problem of grid distortion is due to insufficient accuracy of a second-order difference scheme. Grid stabilizing by incorporating more grid points in the difference operators is due to artificial diffusion analogous to artificial viscosity. The disadvantage of this method is that an effective artificial viscosity is hidden in the equation, usually operating in an unknown way. In some difference schemes a hidden artificial viscosity can be identified by substracting the von Neumann–Richtmyer equations from the difference scheme. The terms left over may then be collected and interpreted in terms of an artificial viscosity.

The approach taken at LRL was to develop a second-order-difference scheme that used the minimum number of grid points and hence had the minimum implicit artificial diffusion. The grid is then stabilized by adding an artificial viscosity to the equations of motion. In this manner the operation of the artificial viscosity is known, and its magnitude can be compared with the magnitude of physical stresses in the problem.

The finite difference operators that replace the partial derivatives are formulated so that they have an important bearing on the physics that the set of partial differential equations is meant to describe. For example, space derivatives are defined as the summation of the normal component of a flux around an enclosed area. Thus, conservation form is introduced into the difference equations. The two-time step and the two-grid system of von Neumann–Richtmyer are employed. One grid system is used to calculate gradients of pressure stresses and the other to calculate the divergence of the velocity vector. The pressure gradients are centered at grid nodes at integral times intervals. The divergence of the velocity is centered at mid-points on the grid at $\frac{1}{2}$-time intervals.

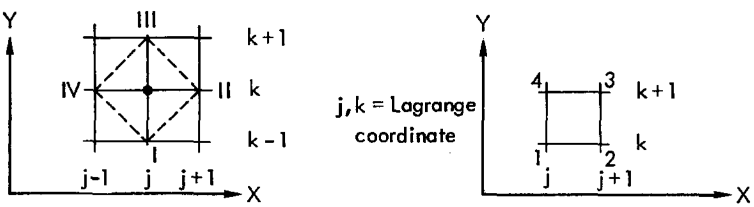

I, II, III, IV Grid for calculating ∇P

P = pressure at time n

1, 2, 3, 4 Grid for calculating $\nabla \cdot \vec{W}$

$\vec{W}$ = velocity at time n + 1/2

The resulting difference equations have these properties: (1) they conserve angular momentum; (2) they transform in the same way as the differential operators. For example, in 2-*D* cartesian coordinates the terms in the difference equations that represent the partial derivatives in the left side of Eq. (1) below will collect and be identically equal to the time centered difference of the quantities on the right side of each equation.

$$
\begin{aligned}
\nabla \cdot \vec{W} &= \frac{\dot{V}}{V} \qquad & W &= \text{velocity vector} \\
& & V &= \text{volume} \qquad\qquad (1)\\
\nabla \times \vec{W} &= \sin \dot{\omega} \qquad & \omega &= \text{angle of rigid rotation.}
\end{aligned}
$$

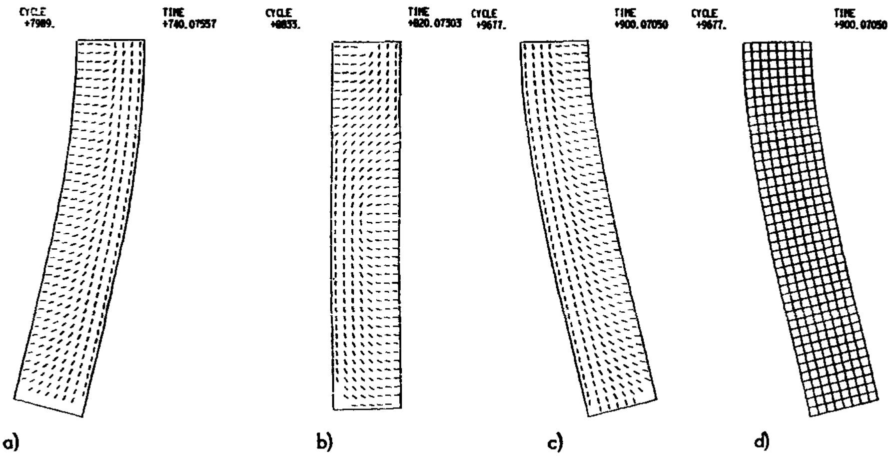

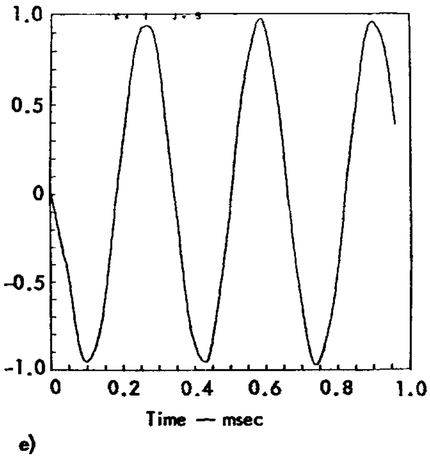

a, b, c) Position of plate at 3 times, μsec. Lines show direction of maximum principal stress. Displacements are multiplied by 10.

d) Lagrange grid at same time as (c).

e) Position-vs-time for a point in the center of the bottom edge.

FIG. 1. Vibration of an elastic plate clamped at the top. Plate length—5.25 cm; plate width—1 cm; density—7.72 g/cm³; bulk modulus—1.88 Mb; shear modulus—0.804 Mb.

This fact leads to zero truncation error in the definition of stress and strain used in the formulation of the elastic-plastic problem.

A computer program (HEMP code) that uses the above difference scheme is described in UCRL-7322 Rev. I. The program has been used for many years at LRL to solve problems in 2-*D* continuum mechanics. The accuracy of the program is $\sim$0.1 % when compared to problems that can be solved by other means. For example, check problems have been done with 2-*D* steady state detonation calculations solved by the method of characteristics and compared with the solution obtained by the time dependent computer program.

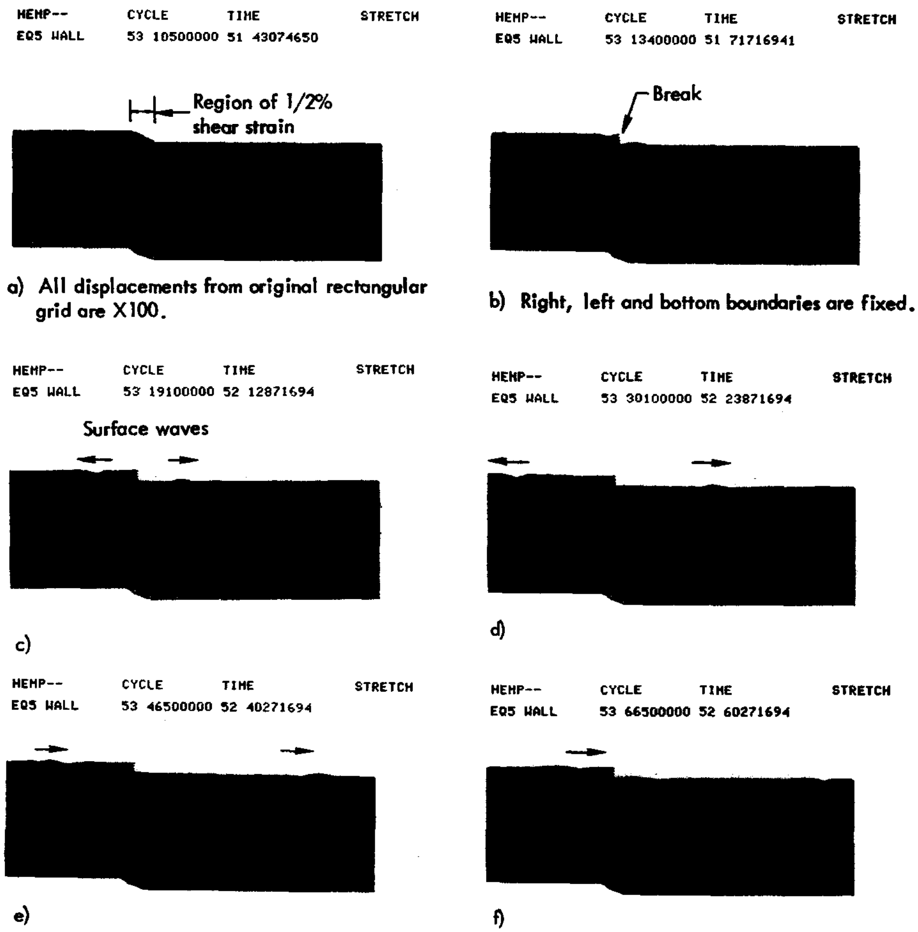

FIG. 2. Surface waves from the release of strain energy in an elastic medium. Bulk modulus—0.4 Mb; shear modulus—0.15 Mb; density—2.5 g/cm^3.

This paper demonstrates the effectiveness of the program for solving a range of physical problems. Examples are given in elasticity, elastic-plastic flow, seismology and gas dynamics.

The first calculation, Fig. 1, shows the vibration of an elastic plate clamped at one end. The plate is set into motion by assigning a velocity $\dot{X} = -10^{-3}$ cm/μ sec to the Lagrange coordinate at the lower right-hand corner and then releasing the velocity after 50 μsec. The plate then oscillates with a period of 320 μsec. This agrees with the fundamental frequency that can be determined from elasticity theory. (See p. 379, Mechanical Vibrations; A. H. Church, John Wiley, 1963.) The calculation was allowed to run for over 10,000 time steps. The wave amplitude and frequency remained constant. The total energy, kinetic plus internal, remained constant to within 0.1 % of the original energy put into the plate. An artificial

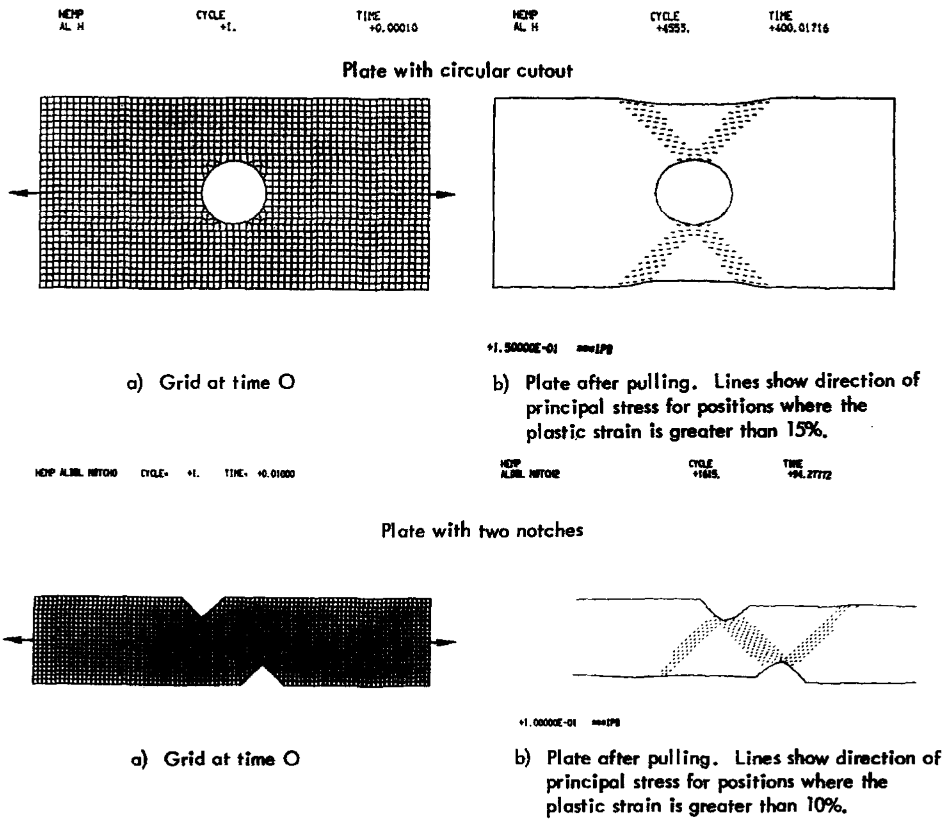

FIG. 3. Tension tests of aluminum plates described by an elastic-plastic equation of state; yield stress: 3 kb. The plates are pulled in the direction of the arrows.

viscosity was used to stabilize the grid. The point here is to show that the physics of the problem was not influenced by the artificial viscosity.

Figure 2 shows a preliminary calculation for studying earthquakes. An initial

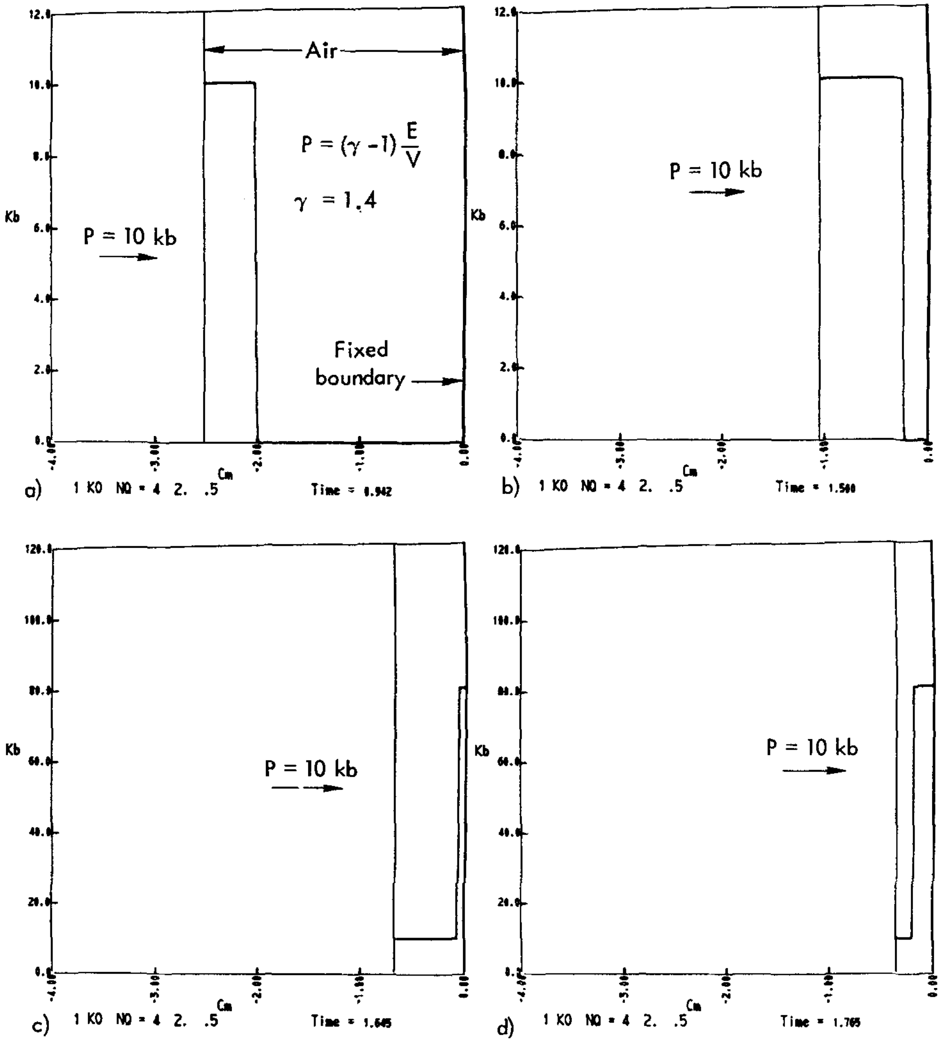

FIG. 4. Pressure, kb, vs position, cm, for a one-dimensional shock induced in air by a constant 10-kb pressure applied at the left boundary.

(a), (b) Incident shock proceeding through the air that was initially between −5.00 and 0.00 cm and at 10^{-3} kb pressure.

(c), (d) 10-kb shock reflects as an 80-kb shock from the fixed boundary at 0.00. Note pressure scale change.

stress field has been introduced into the grid by displacing one part of the grid with respect to the other. The strain energy is released by allowing fracture to occur on a vertical line. The surface waves with the largest amplitudes are travelling at the

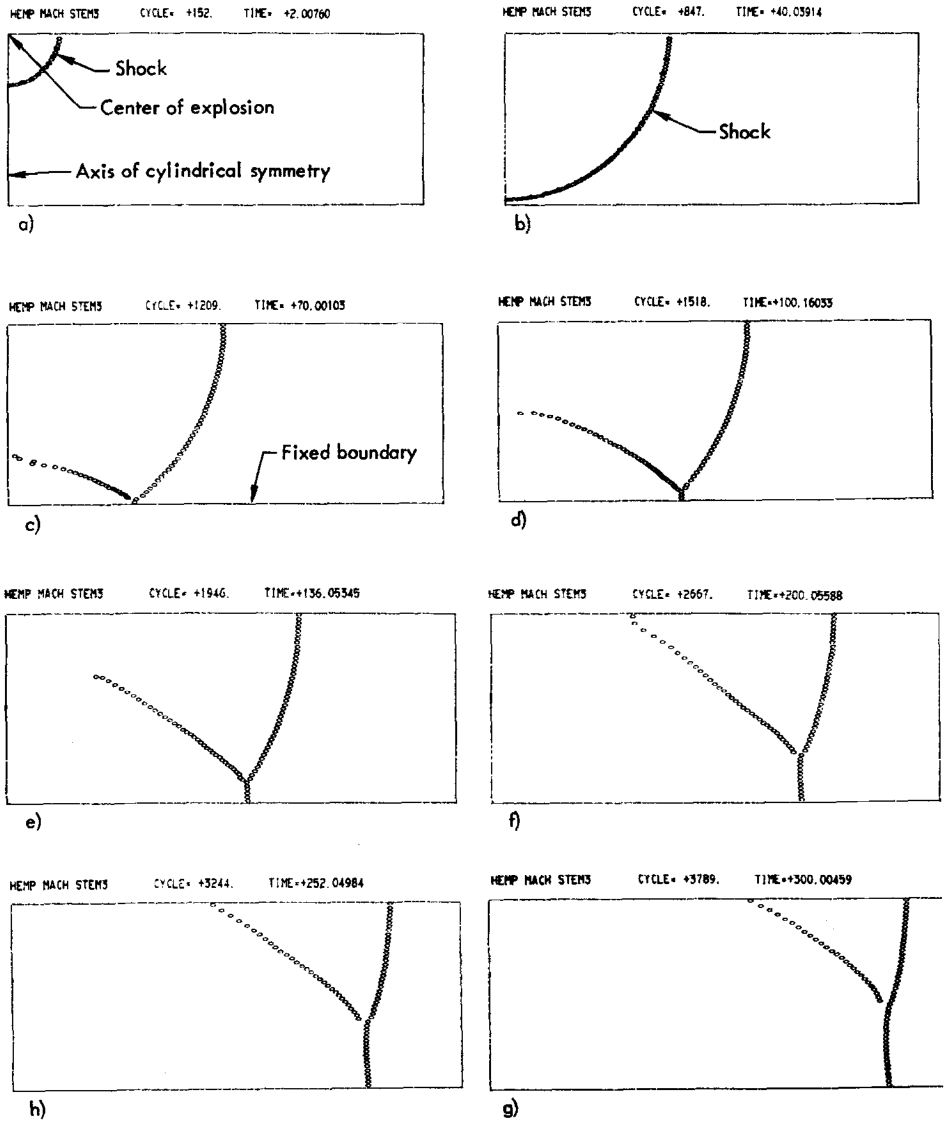

FIG. 5. Mach stem in a $\gamma = 3$ perfect gas produced by the reflection of a spherical wave from a fixed boundary.

velocity of Rayleigh waves. The elastic constants used to describe the material are appropriate for granite.

Figure 3 shows calculations of tension tests for a plate with a circular cut-out and for a plate with two triangular notches. The object here is to demonstrate the difference scheme for problems with irregular boundaries. The equations of state used correspond to aluminum with an elastic yield strength of 3 kb.

Figure 4 shows a calculation of a strong shock proceeding into a gamma law gas and reflecting from a fixed boundary. Reflected pressure is seen to be eight times the incident pressure. This is the correct multiplication factor for a

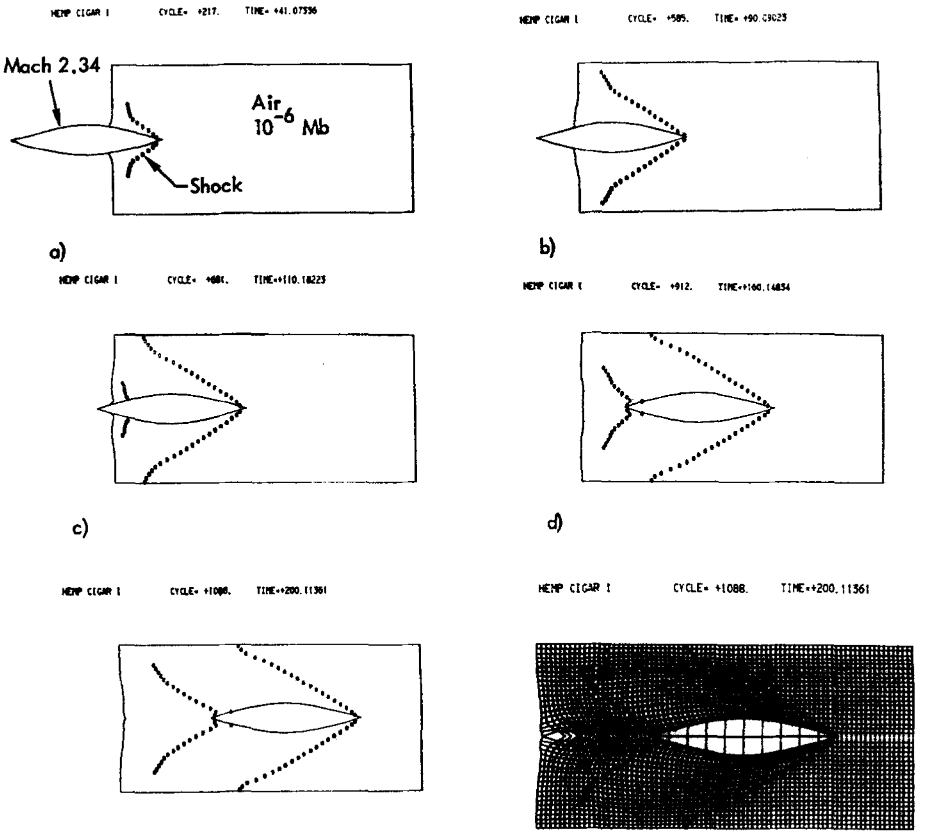

e)

f) Same time as (e) showing the Lagrange grid

FIG. 6. Body with cylindrical symmetry about the long axis moving at Mach 2.34 in air.
(a) → (e)—increasing time, μsec.
(f)—same time as (e) showing the Lagrange grid.

$\gamma = 1.4$ perfect-gas equation of state that can be calculated from the Hugoniot equations. The calculation used a quadratic and a linear artificial viscosity. This problem is a fairly critical test of a computer program to calculate strong shocks in a compressible medium. The pressure profiles shown here were plotted directly on a cathode-ray tube and photographed.

Figure 5 shows the calculation of a Mach stem produced in a $\gamma = 3$ perfect gas by an exploding sphere. A search routine in the computer locates the maximum value of the artificial viscosity in a given space region and plots a circle, thus automatically tracing out the shock space positions. The plots were made on a cathode-ray tube and photographed as described above. Shock positions for the figures that follow were plotted in the same manner.

Figure 6 shows a calculation of a slender body moving at Mach 2.34 through air described by a $\gamma = 1.4$ perfect gas. The initial air pressure inside the calculation grid of the air is one atmosphere. A boundary pressure of one atmosphere is maintained on the right and left sides of the grid representing the air.

Figure 7 shows a calculation similar to the one shown in Figure 6 except that the velocity of the body has been slowed down to a Mach number less than one. It is seen that the bow shock has detached. The shocks behind the slender body are due to reflections from the fixed boundary of cylindrical symmetry.

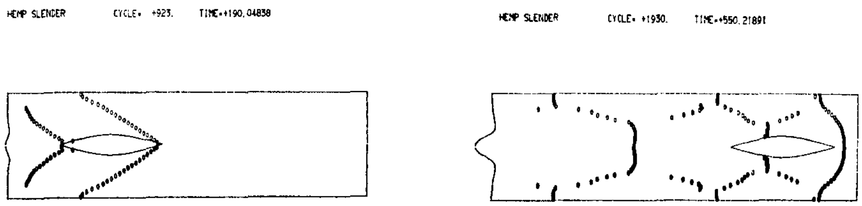

a) Supersonic.

b) Subsonic. Bow shock has detached. Shocks behind the body are from bow shock reflections with the cylindrical boundary.

FIG. 7. Similar to Fig. 6, except the body has been slowed down from Mach 2.34 to Mach 0.8.

ACKNOWLEDGMENTS

The Hemp computer program was programmed by Dick Giroux. Alan Leibee wrote the special routine for tracing out shock positions.

REFERENCES

1. J. VON NEUMANN AND R. D. RICHTMYER, *J. Appl. Phys.* **21** (1950), 232.